Matthew W. Becker[1], Brett Harris[2], Roman Pevzner[2],

[1] Department of Geology, California State University Long Beach, California, USA

[2]WA School of Mines: Minerals, Energy and Chemical Engineering, Curtin University, Perth, Western Australia, Australia

Corresponding Author Matthew Becker, `Matt.Becker@csulb.edu`

Key Points

- Strain and flow direction was correlated or anti-correlated with injection head, depending on injection interval
- Injection and strain behavior was not simply correlated to geophysical or lithologic logs
- Dynamic injection/withdrawal tests are of limited predictive value to managed aquifer recharge

Abstract

The storage of fluids in the subsurface is critical for a broad spectrum of applications including managed aquifer recharge, storage of liquified carbon dioxide and hydrogen, geothermal heat extraction and management of hydrocarbon resources. It is surprising then, that there has been relatively little measurement of the vertical distribution of fluid storage in geologic formations as compared with permeability. We present experiments in which fluid was injected into an important regional aquifer and the depth-dependent strain response measured using fiber optic distributed acoustic sensing. The formation expansion and contraction in response to fluid injection were measured in nanostrain. Strain, and the implied storage distribution, was highly localized in specific strata and demonstrated complex, (non-elastic and non-local) hydromechanical behavior. This new window into fluid-geomechanical coupling undermines some typically use models and observations, currently in practice, but provides potential for complete representation and prediction of fluid storage in the subsurface.

Plain Language Summary

A fiber optic cable was used to measure strain in response to water injection and withdrawal in a sandstone aquifer. The strain was focused in limited strata within the aquifer. In some strata the formation expanded with injection and in others the formation contracted with injection. This complex behavior is attributed to the interaction between fluid flow and mechanical strain in the rock. These results are contrary to common models of water storage which

predict a proportionate expansion of pore space with injection. These results provide important insight into understanding how water is stored and released in aquifers.

Keywords

1828 Groundwater hydraulics, 1822 Geomechanics

Introduction

Efforts to store water (e.g. managed aquifer recharge) and other fluids (e.g. carbon dioxide, liquified hydrogen) in the subsurface are limited by the propensity for the geologic media to accommodate fluid volume through strain. The study of geomechanical strain in response to fluid displacement is generally termed poroelasticity and its theoretical underpinnings are well known (Biot, 1956; Detournay & Cheng, 1993; Wang, 2017). However, the application of theory to real world problems is often limited by the measurement of poroelastic parameters distributed in the subsurface. Volume expansion of pore spaces during injection is most often measured using surface observations with precision GPS (Sun et al., 2020), Interferometric Synthetic Aperture Radar (InSAR), (Galloway & Hoffmann, 2007; Hoffmann et al., 2001; Radutu et al., 2017) and/or tiltmeters (Schuite et al., 2017) . These measurements are based upon the assumption that strain at depth leads to proportional displacement at the surface. As will be shown, this assumption may not be justified because strain is accommodated locally within complex layering of the injection zone.

The recent development of fiber optic sensing techniques has opened new possibilities for understanding depth-distributed strain in the subsurface. Interferometric analysis of backscattered laser light along fiber optic glass can produce displacement of a fiber optic cable in response to geomechanical strain (Lindsey et al., 2020). Depending on the time scale required, two methods are used. For slow strain, distributed strain sensing (DSS) is the method of choice as it can measure distributed strain over periods of days or years (Sun et al., 2020; Zhang et al., 2021). For more rapid strain, distributed acoustic sensing (DAS) is the method of choice as it can measure strains at frequencies in the 10's of kHz (Becker et al., 2020). Both methods can collect information at meter or sub-meter intervals over many kilometers. However, current DSS interrogators can resolve strains approaching 1 microstrain, while DAS interrogators have potential to resolve strains exceeding 1 nanostrain at frequencies of 1 mHz and higher.

We document spatially distributed and dynamic measurements of the poroelastic response to water injection and withdrawal from a single deep well. Fiber optic DAS provided unprecedented detail in the strain behavior over a 235 m interval of a prolific sandstone aquifer. The depth-distributed strain measurements revealed poroelastic behaviors that are more spatially and temporally complex than previously expected for stratified bedrock formations. These responses may warrant re-thinking of how fluid injection is monitored in geologic reservoirs.

Methods

Field Site

Experiments were conducted at the Curtin National Geosequestration Laboratory (NGL) research facility located on the main campus of Curtin University in Perth Australia. The NGLd borehole targets the regionally important Yarragadee aquifer (Pujol et al., 2015; Torkzaban et al., 2015). The Yarragadee Aquifer is composed of the Gage and Yarragadee formations and is fine- to medium-grained sandstone interbedded with mudstones and siltstones. Although the formation is lithified, the conductive porosity is probably primary, i.e. not dominated by fractures. The NGL well is constructed with fiberglass casing that is screened between 653 and 888 m depth below the surface (**Figure S3**). The top of the Yarragadee formation is at about 671 m below the surface and the bottom is thought to be more than 1700 m deep (Pujol et al., 2015). Below 380 m depth, the annulus between the 180 mm outer diameter of the well casing and the 311 mm diameter of the borehole is filled with a graded sand (Rockwater Hydrogeological and Environmental Consultants, 2016).

Hydraulic Testing

The hydraulic stress on the aquifer was imparted by moving a solid cylinder up and down across the water level in the well. As the cylinder, or "slug" as it is known in the hydrogeology community, was oscillated it displaced water in the well causing the hydraulic head in the well to oscillate. The elevated or depressed head in the well pushed or pulled water from the aquifer, respectively, causing strain in the formation surrounding the well. The slug was constructed of an approximately 3 m long 0.1 m diameter PVC pipe. It was suspended on a low-stretch rope connected to a tripod and driven by an electric hoist. Autonomous pressure loggers (Dipperlog-32, Heron Instruments, Ontario, Canada) were lowered into the well and affixed to the bottom of the slug to allow calculation of injected volume and flow rate. When oscillated, the maximum volume of water injected into the formation by the slug was approximately 14 liters. The injection rate varied based upon the period of oscillation.

When a long water column in a well is rapidly displaced by a slug, the inertial force of the water column affects the injection. This "underdamped" condition is well known in hydrogeology, and mathematical solutions are available for interpreting the head response at the well. The head recover after slug insertion was very well represented by the appropriate analytic solution (Butler Jr & Zhan, 2004), resulting an estimated bulk hydraulic conductivity (K) of 8.3e-6 m/s and specific storage = 1.5e-9 m^{-1} (**Figure S2**).

For reference, the radial distance from a well over which a formation is interrogated by slug test can be calculated assuming simple radial flow in a homogeneous formation. Under these idealized conditions, the radial distance of hydraulic penetration (radius of influence) is a function of the hydraulic diffusivity (D) and the period (P) over which the formation is strained hydraulically. *Bakker* (2009) defines a characteristic length scale of penetration as $\lambda = \sqrt{DP/2\pi}$. The amplitude of the hydraulic signal is expected attenuated by a factor of 10 will be 1.78 λ. The hydraulic diffusivity is the ratio of the hydraulic conductivity to the specific storage ($D = K/S_s$), which is 5400 m^2/sec based upon these slug test estimates. For the period of injection of the slug, which lasts about 30 seconds, the radius of penetration is estimated to be about 290 m. The hydraulic response is expected, consequently, to extend far beyond the borehole.

DAS Acquisition

Distributed acoustic sensing (DAS) uses the interference of backscattered laser light to measure strain. If $u(z,t)$ is the dynamic displacement of a point, z, in the fiber at time, t, then the following measurements are equivalent(Daley et al., 2016)

$\frac{\partial v}{\partial z} = \frac{\partial \epsilon}{\partial t}$ (1)

where v is displacement rate or velocity ($\partial u/\partial t$) and ϵ is strain ($\partial u/\partial z$). The instrument used in this study (iDAS v2, Silixa LTD, London, UK) measures the *relative* displacement rate at two positions separated by a gauge length, L, i.e. $v(z+L,t)-v(z,t)$. Strain rate is then calculated by dividing the relative displacement rate by L. Strain along the fiber, ϵ_z, is computed by integrating through time. Previous researchers have used a similar technology, distributed strain sensing (DSS) to monitor aquifer strains in response to injection and pumping (Zhang et al., 2021). DSS, however, is sensitive to around 1 microstrain, while DAS was able to resolve 1 nanostrain in our experiments.

The gauge length of DAS inherently limits the spatial resolution of the displacement measurements. A displacement at a single point in the fiber would appear as a 10 m wide two-sided step (tophat) in the distributed displacement signal (Becker et al., 2020). Consequently, the observed heterogeneity of strain is smeared with respect to the true heterogeneity in these experiments. With a 235 m zone of observation, however, the spatial distribution of formation displacement in response to injection is highly informative.

The fiber optic cable installed in the borehole is an armored loose-tube cable carrying single and multimode fibers, which are housed in individual plastic buffer tubes filled with gel. The cable was strapped onto the fiberglass casing as it was lowered into the well. The annulus between the casing and the borehole was packed with sand and gravel in the permeable zone and cemented above. The tight packing of sand provides the mechanical coupling necessary to measure formation strain (Becker et al., 2020).

Measured Strain Response

The DAS instrument recorded large displacement rates along the fiber in the interval screened in the Yarragadee aquifer (**Figure 1**). It also recorded significantly smaller displacement rates at a depth interval of about 550 to 570 m corresponding to the depth of pressure actuated cementing ports designed to cement an interval above open area screens. The interval from 785 to 885 m depth shows limited strain response. This interval corresponds with a thicker uniform silt and fine sand dominated package (**Figure S1**).

Figure 1 shows the distributed strain rate (nanostrain/sec) during a short injection. Injection is carried out by displacing fluid using a long solid cylinder (slug). As the slug is lowered in the well, water level rises as water is simultaneously forced into the formation, resulting in a measurable strain. In Figure 1, expansion of the formation (positive strain rate) is shown in red while contraction (negative strain rate) is shown in blue. There is a brief lag between head increase and formation strain response. At specific depths (e.g. ~714 m) the formation expands with head rise in the well and contracts as the water level declines. At other depths (e.g. ~732 m) the opposite response occurs. The overall picture is that storage is highly distributed, occurring in or due to compressive strata bordering more permeable units.

The poroelastic response is repeatable. **Figure 2** shows vertical strain (integrated through time from strain rate) for a test (Test 28) in which the slug was oscillated up and down in the well at a period of 40 seconds. The resulting strain amplitudes varied over an order-of-magnitude with depth. For example, amplitudes at 714 and 851 m were about 1200 and 90 nanostrain, respectively. Strain measurements were well above noise at approximately one nanostrain.

Strain rate is a more relevant measurement to compare with fluid injection based upon continuum concepts (Equation 2). The observed strain rate, and therefore fluid movement in the formation, does not respond simply to the oscillating hydraulic head in the injection well. As an example, strain rate measured at depths of 732 and 773 m are compared with total pressure head in the injection well in **Figure 3**. At 732 m, the strain rate is positively correlated with well head, but the signal is not symmetric, (i.e., non-elastic). Fluid interacts differently with the pore space during injection than withdrawal. The strain rate at 732 m is anticorrelated with well heads indicating contraction as water is forced into adjacent units.

Interpretation with Respect to Poroelastic Models

Distributed strain measured in this borehole indicates that "poroelastic" storage is generally non-elastic and shown to be localized across specific depths zones over the screened interval where there is hydraulic communication with the aquifer. Active intervals have thicknesses of about 10 m according to the strain rate profile (**Figure 3**) but the real thickness of intervals may be smaller. The DAS instrument measures strain rate(Daley et al., 2016) through the relative displacement rates of two points along the fiber divided by a 10 m gauge length (see Methods). This means that two hydrostratigraphic features within a 10 m interval cannot be distinguished. However, the spatial resolution is good relative to the 235 m screened interval, illustrating how fluid flow and storage is dominated by relatively short intervals in the 240 m screened zone.

The fact that strata are alternately compressive and expansive implies that it is possible that water is moving into the aquifer at some depths and out at others, under the same driving head gradient. Such reverse water flow has been observed at aquifer scale where a confining unit can exhibit an opposite change in head when compared with the aquifer units which it confines (Burbey, 2013; Hsieh, 1996; Slack et al., 2013). This behavior is referred to as the "Noordbergum effect" and is generally attributed to the offset in time between mechanical and fluid transfer of strain in the formation (Wang, 2017, Sect 9.3). Although distributed pressure is not measured in this experiment, the distributed strain is consistent with a dynamic and three dimensional poroelastic response in the vicinity of the well bore.

Strain-rate and fluid flow are related through fluid and mechanical continuity. The three-dimensional coupling of fluid flow and time variation of volumetric strain can be represented by the equation:

$\alpha \frac{\partial \epsilon_{\mathrm{kk}}}{\mathrm{dt}} + S_\epsilon \gamma \frac{\partial h}{\partial t} = -\nabla \bullet \tilde{q}$, (2)

where α is the Biot-Willis coefficient, γ is the specific weight of water, h is hydraulic head, and $\tilde{q}$ is the specific discharge vector (Wang, 2017, eq. 4.65). The volumetric strain, ϵ_{kk}, is expressed here in index notation and implies that the volumetric strain is equal to the divergence of displacement. The specific storage at constant strain, $S_\epsilon\gamma$, is similar to the specific storage coefficient typically used in hydrogeology, except that is subject to constant strain condition instead of constant stress, i.e. $S_s = S_\sigma\gamma$. The two may be related by $S_\epsilon = S_\sigma - \alpha^2/K$, where K is the drained bulk modulus (Wang, 2017, eq. 3.38). For simplicity of presentation here, however, S_ϵ is substituted for S_σ with the recognition that $S_\epsilon < S_\sigma$.

The two left hand terms in Equation (2) represent the different storage types present in the formation. The term $\frac{\partial\epsilon_{kk}}{\partial t}$ represents water storage due to volume change of the formation, while the term, $S_\epsilon\gamma\frac{\partial h_\epsilon}{\partial t}$, represents water released from compressibility of formation and fluid. In typical models of groundwater flow the first term is ignored and storage is expected to be proportional to change in hydraulic head. DAS measures uniaxial strain rate the formation $\frac{\partial\epsilon_{zz}}{\partial t}$, rather than volumetric strain, but clearly these measurements indicate that fluid storage is dominated by locally variable volumetric storage.

Furthermore, the fact that the strain-rate plateaus as the slug is removed from the well at some depths (e.g. 713 m, **Figure 3**) suggests that there is exchange of water among strata and it is not reversed when the flow from the well reverses. Water movement near the well is, therefore, not strictly radial as is often assumed in well hydraulics. Three-dimensional fluid movement is not contrary to poroelastic theory, but is contrary to current practice in well testing. De Simone and Carrera(De Simone & Carrera, 2017) used numerical modeling to argue that non local and reverse flow can occur in formations which are not hydromechanically constrained

Conclusions

The distributed strain measurement in response to hydraulic perturbation in this well suggest that (1) injection into the formation is highly heterogeneous, (2) strain response is non-elastic, (3) strain response is non-local with adjacent strata interacting poroelastically. The first finding has been often observed in stratified aquifers through geophysical flow logging and in itself is not surprising. The non-elastic and non-radial response of aquifer material to pressure (i.e. **Figure 3**) has not been observed previously in a depth-distributed manner. *Sun et al.* (2020) measured distributed strain in response to injection in a nearby well, but the perforated intervals were too short (2 m) to reveal interaction between stratigraphic units of varying permeability and mechanical compliance.

The non-elastic strain responses are usually attributed to plastic deformation which is expected over long time periods or large stresses. These tests were neither long nor introduced large volumes of fluid. Asymmetric strain responses have been observed near wells using strain meters installed across crystalline bedrock fractures (Schweisinger et al., 2011). The non-elastic responses were attributed to non-local behavior of deformation. *Vinci et al.* (2015) provided theoretical interpretations of this kind of behavior in bedrock fractures.

Although storage as a property is often assumed to be homogeneous within strata, it has long been recognized that storage is constant neither in time nor space (Verruijt, 1969). Some analytic solutions have been presented to account for non-local deformation with simplified flow geometries (De Simone & Carrera, 2017). More widely available are numerical treatments of non-local storage (Berg et al., 2011; Hsieh, 1996; Yin et al., 2007). We are unaware of any previous field data that support models of non-local flow in formations that are dominated by porous rather than fractured flow, as is shown from our experiments in the Yarragadee Aquifer.

Fiber optic distributed strain sensing (either DAS or DSS) will no doubt continue to unlock new understand of poroelastic behavior in geologic formations. Distributed strain in response to injection has already been demonstrated in bedrock fracture networks (Becker et al., 2020) and in aquifers (Sun et al., 2020). Still needed are distributed poroelastic strains measured in porous formations at variable distances from an injection and pumping well. Our conclusions are based on measurements of near borehole response from a deep research well instrumented with fiber optic cable.

As advancements in field measurements, poroelastic theory, and numerical modeling progress, it is likely that treatments of geofluid systems will move away from traditional local elastic response models and toward a distributed hydromechanical approach. Fully coupled hydromechanical approaches can account for of the range of behaviors observed in these experiments. In the meantime, vertically integrated approaches that use surface deformation to directly observe fluid storage should be viewed with a critical eye in stratified porous formations.

Acknowledgements

The authors wish to acknowledge the support of the United States-Australia Fulbright Program. The NGL test site is supported through ANLEC R&D, supported by Low Emission Technology Australia and the Australian Government through the Department of Industry, Science, Energy and Resources; the Victorian Government, BHP, the Commonwealth Government via the EIF, and the CO2CRC members who have committed their time and support to the Stage 3 Project. Preliminary experiments with DAS were supported by the National Science Foundation under Grant MRI-1920334.

Open Research

Data and Matlab scripts used to generate figures in this article may be found at:

Becker, M., Harris, B., & Pevzner, R. (2022). Data and Matlab scripts for article "Distributed Water Storage Measured by Fiber Optic Distributed Acoustic Sensing" submitted to Geophysical Research Letters by Becker, Harris, Pevzner [Data set]. Curtin University. https://doi.org/10.25917/BGFS-NR77

Figures

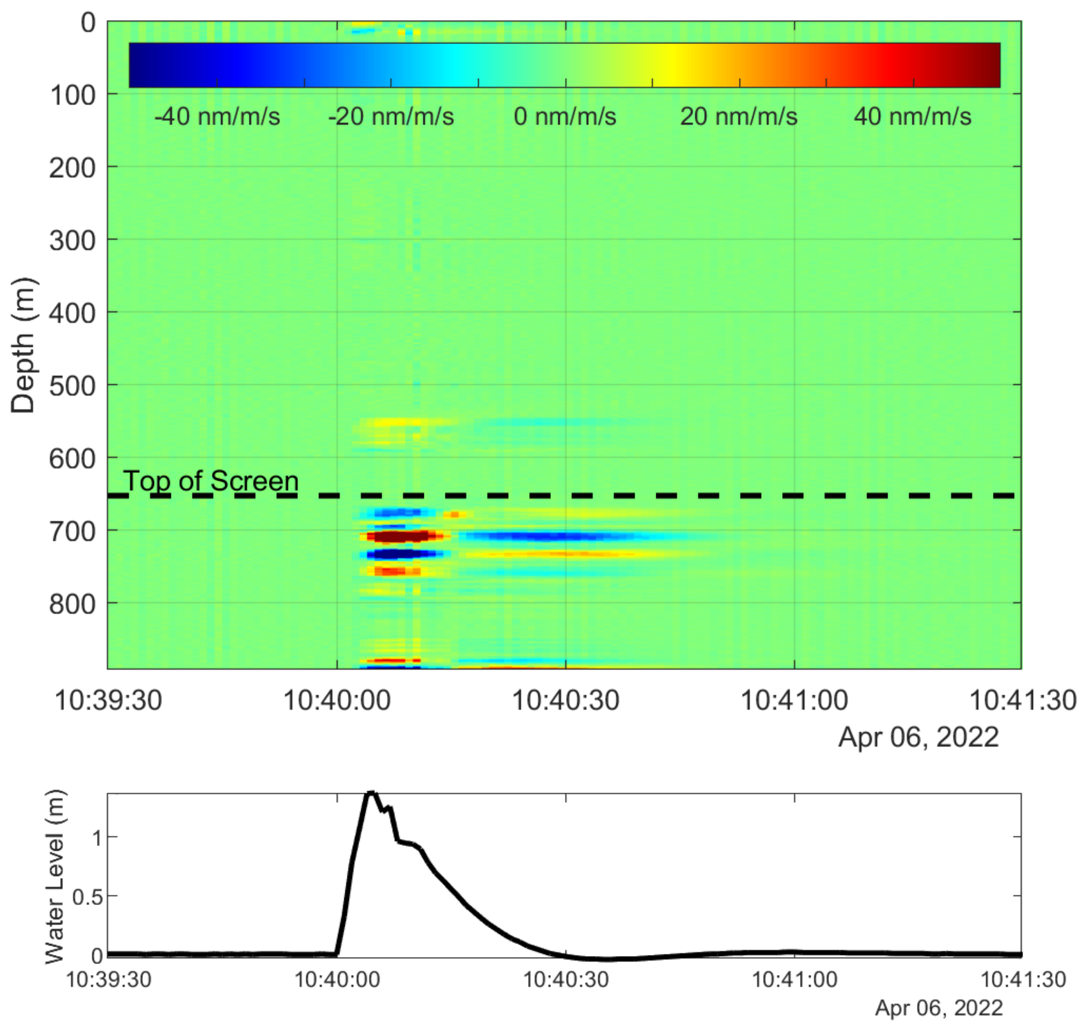

Figure 1. DAS measured strain response to slug insertion (upper) compared to change in water level measured in well (lower). Water levels are continuously

measured with a pressure transducer located at XX in the well column. Large positive and negative changes in strain are measured along the screened interval via DAS with fiber optic cable permanently attached to the outside of the NTL injection well casing.

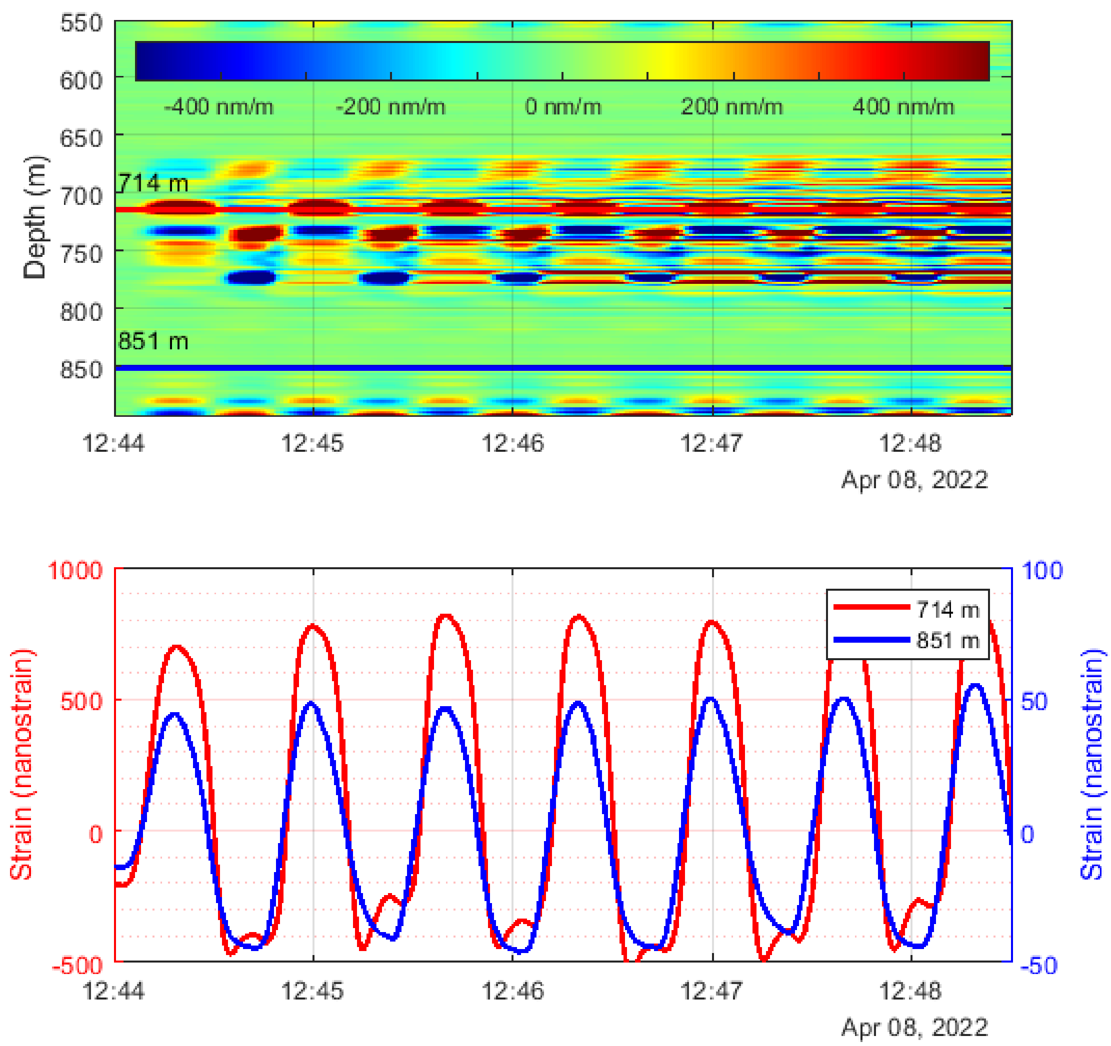

Figure 2. Comparison of strain in more responsive (red) and less responsive (blue) strata. Strain rate is significantly different in each layer as the layers are expected to have marked differences in poro-elastic properties.

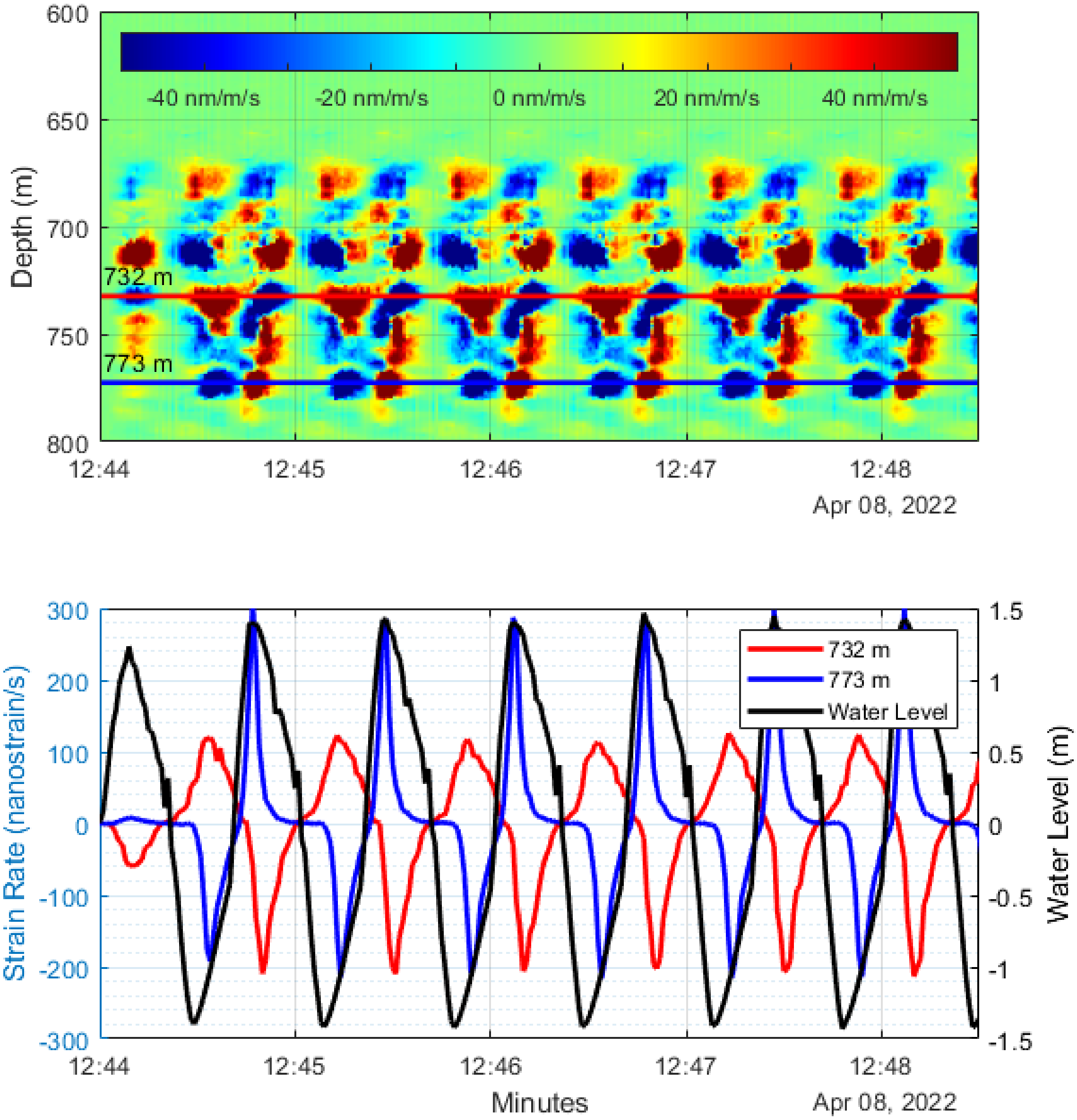

Figure 3. Strain rate in responsive zone that are correlated (red) and anticorrelated (blue) with change in water level measured in the well (black curves referenced to the right-hand water level axis) This test shows excellent repeata-

bility through cycles and significant differences in the DAS strain rate recovered from the two depths.

References

https://agupubs.onlinelibrary.wiley.com/doi/abs/10.1029/2020WR028140

https://ngwa.onlinelibrary.wiley.com/doi/abs/10.1111/j.1745-6584.2010.00781.x

https://onlinelibrary.wiley.com/doi/abs/10.1111/1365-2478.12324

https://agupubs.onlinelibrary.wiley.com/doi/abs/10.1002/2017WR020824

https://doi.org/10.1007/s10040-006-0121-5

https://agupubs.onlinelibrary.wiley.com/doi/abs/10.1029/2019JB018145

https://www.sciencedirect.com/science/article/pii/S0375650515000565

https://www.sciencedirect.com/science/article/pii/S1877705817361404

https://agupubs.onlinelibrary.wiley.com/doi/abs/10.1002/wrcr.20095

https://agupubs.onlinelibrary.wiley.com/doi/abs/10.1029/2019WR024794

https://www.sciencedirect.com/science/article/pii/S0169772215000881

http://gji.oxfordjournals.org/content/202/3/1613.abstract

Bakker, M. (2009). Sinusoidal pumping of groundwater near cylindrical inhomogeneities. *Journal of Engineering Mathematics, 64*(2), 131-143. Becker, M. W., Coleman, T. I., & Ciervo, C. C. (2020). Distributed Acoustic Sensing as a Distributed Hydraulic Sensor in Fractured Bedrock. *Water Resources Research, 56*(9), e2020WR028140. Berg, S. J., Hsieh, P. A., & Illman, W. A. (2011). Estimating Hydraulic Parameters When Poroelastic Effects Are Significant. *Groundwater, 49*(6), 815-829. Biot, M. A. (1956). Theory of Propagation of Elastic Waves in a Fluid-Saturated Porous Solid. I. Low-Frequency Range. *The Journal of the Acoustical Society of America, 28*(2), 168-178. Burbey, T. J. (2013). Poroelastic Effects on Fracture Characterization. *Groundwater, 51*(6), 904-913. Butler Jr, J. J., & Zhan, X. (2004). Hydraulic tests in highly permeable aquifers. *Water Resources Research, 40*(12). Daley, T. M., Miller, D. E., Dodds, K., Cook, P., & Freifeld, B. M. (2016). Field testing of modular borehole monitoring with simultaneous distributed acoustic sensing and geophone vertical seismic profiles at Citronelle, Alabama. *Geophysical Prospecting, 64*(5), 1318-1334. De Simone, S., & Carrera, J. (2017). Analytical Solutions to Coupled HM Problems to Highlight the Nonlocal Nature of Aquifer Storage. *Water Resources Research, 53*(11), 9580-9599. Detournay, E., & Cheng, A. H. D. (1993). 5 - Fundamentals of Poroelasticity. In C. Fairhurst (Ed.), *Analysis* *and Design Methods* (pp. 113-171). Oxford: Pergamon.Galloway, D. L., & Hoffmann, J. (2007). The application of satellite differential SAR interferometry-derived ground displacements in hydrogeology. *Hydrogeology Journal, 15*(1), 133-154. Hoffmann, J., Zebker, H. A., Galloway, D. L., & Amelung, F. (2001). Seasonal subsidence and rebound in Las Vegas Valley, Nevada, observed by synthetic aperture radar interferometry. *Water Resources Research, 37*(6), 1551-1566. Hsieh, P. A. (1996). Deformation-induced changes in hydraulic head during ground-water withdrawal. *Groundwater, 34*(6), 1082-1089. Lindsey, N. J., Rademacher, H., & Ajo-Franklin, J. B. (2020). On the Broadband Instrument Response of Fiber-Optic DAS Arrays. *Journal of Geophysical Research: Solid Earth, 125*(2), e2019JB018145. Pujol, M., Ricard, L. P., & Bolton, G. (2015). 20 years of exploitation of the Yarragadee aquifer in the Perth Basin of Western Australia for direct-use of geothermal heat. *Geothermics, 57*, 39-55. Radutu, A., Nedelcu, I., & Gogu, C. R. (2017). An overview of ground surface displacements generated by groundwater dynamics, revealed by InSAR techniques. *Procedia Engineering, 209*, 119-126. Rockwater Hydrogeological and Environmental Consultants. (2016). *Yarragadee aquifer geophysical instrument calibration bore completion report, prepared of the National Geosequestration Laboratory, Curtin University, Perth, Western Australia, Australia*. Retrieved from Schuite, J., Longuevergne, L., Bour, O., Guihéneuf, N., Becker, M. W., Cole, M., et al. (2017). Combining periodic hydraulic tests and surface tilt measurements to explore in situ fracture hydromechanics. *Journal of Geophysical Research: Solid Earth*. Schweisinger, T., Svenson, E. J., & Murdoch, L. C. (2011). Hydromechanical behavior during constant-rate pumping tests in fractured gneiss. *Hydrogeology Journal, 19*(5), 963-980. Slack, T. Z., Murdoch, L. C., Germanovich, L. N., & Hisz, D. B. (2013). Reverse water-level change during interference slug tests in fractured rock. *Water Resources Research, 49*(3), 1552-1567. Sun, Y., Xue, Z., Hashimoto, T., Lei, X., & Zhang, Y. (2020). Distributed Fiber Optic Sensing System for Well-Based Monitoring Water Injection Tests—A Geomechanical Responses Perspective. *Water Resources Research, 56*(1), e2019WR024794. Torkzaban, S., Bradford, S. A., Vanderzalm, J. L., Patterson, B. M., Harris, B., & Prommer, H. (2015). Colloid release and clogging in porous media: Effects of solution ionic strength and flow velocity. *Journal of Contaminant Hydrology, 181*, 161-171. Verruijt, A. (1969). Elastic Storage of Aquifers, in: Flow through Porous Media (R.J.M. De Wiest, editor), Academic Press, New York, 1969, 331-376. In (pp. 331-376).Vinci, C., Steeb, H., & Renner, J. (2015). The imprint of hydro-mechanics of fractures in periodic pumping tests. *Geophysical Journal International, 202*(3), 1613-1626. Wang, H. F. (2017). *Theory of linear poroelasticity with applications to geomechanics and hydrogeology*: Princeton University Press.Yin, S., Dusseault, M. B., & Rothenburg, L. (2007). Coupled multiphase poroelastic analysis of reservoir depletion including surrounding strata. *International Journal of Rock Mechanics and Mining Sciences, 44*(5), 758-766. Zhang, Y., Lei, X., Hashimoto, T., & Xue, Z. (2021). Toward Retrieving Distributed Aquifer Hydraulic Parameters From Distributed Strain Sensing. *Journal of geophysical research. Solid earth, 126*(1), n/a.